Chiang Mai J. Sci. 2017; 44(4) : 1570-1582
http://epg.science.cmu.ac.th/ejournal/
Contributed Paper

Response Surface Methodology Based Optimized Purification of the Residual Glycerol from Biodiesel Production Process

Muhammad Danish* [a], Muhammad Waseem Mumtaz [a], Mahpara Fakhar [a] and Umer Rashid* [b]

[a] Department of Chemistry, Faculty of Science, University of Gujrat, Gujrat-50700, Pakistan.

[b] Institute of Advanced Technology, Universiti Putra Malaysia, 43400 UPM Serdang, Selangor, Malaysia.

*Author for correspondence; e-mail: drdanish62@gmail.com; umer.rashid@yahoo.com

Received: 15 September 2015
Accepted: 15 December 2015

ABSTRACT

Biodiesel is gaining acceptance as an alternative source of energy, due to its important properties, renewability, less toxicity and environmentally friendly attributes. One of the constrains, associated with the use of biodiesel as fuel is its high price. The most promising way to make it cost effective is the purification and utilization of its by-product glycerol. During the refining of glycerol, the following sequence was followed: acidification, neutralization, solvent extraction and decolorization. Optimized conditions for getting a high yield refined product were attained using the response surface methodology (RSM) for different parameters such as pH 1; extraction temperature, 50 °C; extraction time, 40 min; activated carbon dose, 2.0 g and rate of shaking, 350 rpm. Furthermore, the refined glycerol was characterized such as density, 1.65g/cm^3; specific gravity, 1.23; ash content, 1.06; refractive index, 1.05 and pH, 6.05. Raman and FTIR spectroscopic methods were used for the monitoring of glycerol purification.

Keywords: residual glycerol, purification, RSM, characterization

1. INTRODUCTION

The current situation of fuel discrepancy has forced both the developed and developing countries alike to focus on some alternative fuels [1, 2]. These days, biodiesel as an alternative fuel is gaining much importance, being technically compatible with conventional diesel and having additional benefits, *i.e.,* renewable and eco-friendly nature [3,4]. The most accepted method for the synthesis of biodiesel is the transesterification of the feedstock of biological origin. Biodiesel can be produced from various vegetable oils like soybean oil, cottonseed oil, sunflower oil, rapeseed oil, linseed oil, Jatropha oil etc. Transesterification is preceded either by an acid catalyzed or base catalyzed process (Scheme-1) [5]

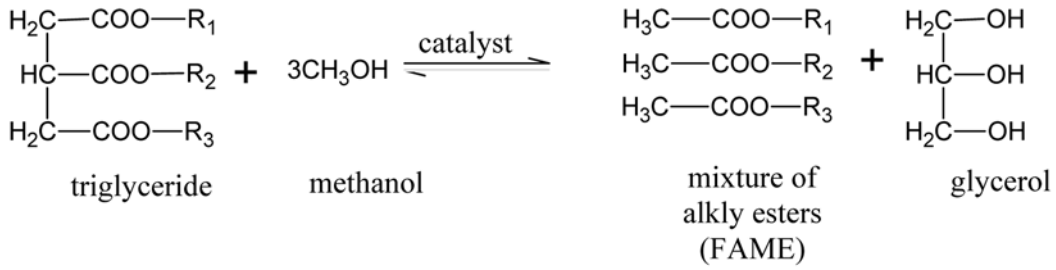

R_1, R_2, R_3 = Hydrocarbon chain ranging from 15 to 21 carbonatoms

Scheme 1. Transesterification reaction of a triacylglycerol.

Glycerol, a by-product of the transesterification process, with all other accumulated components, forms the glycerin phase, and is known as G-phase or crude glycerol [6]. The percentage of glycerin which is produced as a by-product of the reaction is approximately 10% of the feedstock [7]. The crude glycerol directly discharged contaminates the environment as it also contains various other chemicals [8]. Different techniques, such as vacuum distillation, neutralization, electrochemical, solvent extraction and adsorption, have been applied to purify the crude glycerol [9]. The refined glycerol has been used in wetting agents, emulsifiers, detergents, paper and pulp, asphalt (mixture of sand and tar), photographic products, tobacco processing, leather and textile industries [10-15].

The presented work was therefore planned to optimize the stepwise refining and purification protocol of residual glycerol from biodiesel production process by using response surface methodology(RSM). Furthermore, analytical characterization of refined glycerol for its quality evaluation has also been performed.

2. MATERIALS AND METHODS

2.1 Procurement of Raw Material

Glycerol was obtained from the Chemistry Laboratory, University of Gujrat, Gujrat, Pakistan, that utilizes waste oil as the untreated material for biodiesel production via the alkali based transesterification process. All the reagents and chemicals (98% of sulphuric acid, methanol, sodium hydroxide and diethyl ether, KOH, HCl, acetone) used in the current study were of analytical/research grade obtained from Merck Chemicals, Darmstadt, Germany. All experiments were performed thrice and the results presented as mean values along with their standard deviations.

2.2 Physico-chemical Characterization of Crude Glycerol

The crude glycerol procured for the purification purpose was physico-chemically characterized, estimating quality parameters including pH, color, ash content, refractive index, density, specific gravity and surface tension etc., using ASTM standard analytical methods.

2.3 Purification of Waste Glycerol

Waste glycerol was purified by acidification followed by layer formation, neutralization, solvent extraction and adsorption treatments. In the acidification step, the crude sample was treated using H_2SO_4. After the acidification step, the reaction mixture was left to settle down for at least 24 hrs. During this period, the mixture separated into three layers viz a top layer consisting of esters fats, middle layer of

acidified glycerol and lower layer of an aqueous solution of salts. The glycerol layer was separated and heated on a heating plate in a temperature range of 30-50 °C with a constant stirring (using magnet bar). In the neutralization step, the sample was treated with 50% NaOH to pH 7. This step of the purification protocol is considered very vital to get a high quality of refined glycerol. In the solvent extraction step, the processed glycerol was extracted in methanol and chilled for 30 min in a refrigerator to precipitate the traces of inorganic salts. After chilling and filtration the processed glycerol was further treated with activated carbon to remove colored impurities and again filtered. Different doses of activated carbon produced different yields and quality of the refined glycerol. In the last step the processed glycerol was subjected to vacuum distillation [16, 17]. The flow of protocol used for the purification of glycerol residue is displayed in Figure1.

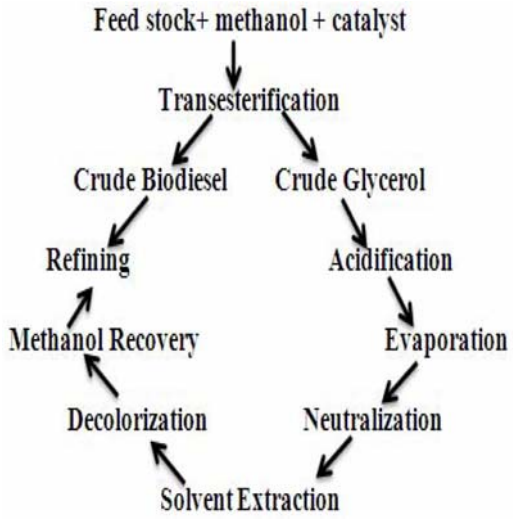

Figure 1. Schematic diagram of protocol used for the purification of glycerol residue.

2.4 Experimental Design for Optimization of Glycerol Purification

Different variables like pH during acidification (A), glycerol extraction time (B), glycerol extraction temperature (C), rate of shaking during extraction (D), dose of activated carbon (E), that affect the percent yield, were optimized using Central Composite Response Surface Design (CCRD) [5]. The under study variables i.e., A, B, C, D and E ranged from 1-5 pH, 20-60 minutes, 30-50 °C, 200-500 rpm and 20-250 g. CCRD, were used in the design to analyze each factor by performing 50 experiments, each repeated in triplicate.

2.5 Statistical Analysis and Selection of Suitable Model

The design expert 7 and SPSS software were used for the Analysis of Variance (ANOVA), response surface, contour plots and diagnostic checks. The mathematical model for the experimental design was selected on the basis of p value with high statistical significance, lack of fit test and high value of R^2. F-test and T-test were used to check the significance of the selected model and individual coefficients. The necessary hypothesis for the validity of the model was checked by diagnostics, such as the normal probability plot. Contour and response surface plots were used to obtain the combination of the levels of the variables for the optimum yield of the refined glycerol.

2.6 FT-IR and Raman Spectroscopy of Crude and Refined Glycerol

Monitoring of the purification from crude to refined glycerin was carried out with the help of the FTIR analysis. The Carry 660 FTIR spectrophotometer made by

'Agilent Technologies' was used for the analysis of the refined glycerol. The FTIR analysis of the crude and refined glycerol was performed by using Diamond Crystal over a scanning range of 4000-650 cm^{-1}. Whereas, Raman Spectrometry was performed using Raman Spectrometer (HORIBA) with a He-Ne laser source, 632.8 nm wavelength, spectral resolution of 1 per centimeter and a CCD CEMERA as a detector.

3. RESULTS AND DISCUSSION

The presented work compiles the output of the research carried out to optimize the purification process of glycerol, a by-product of the biodiesel synthesis process, using RSM. Certain reaction parameters that have significant impact on the purification process have also been optimized. The features which were optimized include: pH, reaction temperature, glycerol extraction time, rate of shaking (RPM), activated carbon dose (g) etc.

3.1 Purification of Crude Glycerol and Physico-chemical Characteristics

The purification of the crude glycerol was carried out as per the defined methodology with the following observations: in the acidification step, it was observed that a high amount of acid will lead to a high proportion of impurity separation as reported by Hunsom et al. [18]. It was also observed that the whole mixture consisted of three layers including esters, crude glycerol, fatty acids and salts. These layers were separated by using different separation methodologies as reported by Wall, et al. [19]. In the neutralization step, the acidified sample was neutralized with 50% NaOH and the inorganic salts were separated in a large amount similar to the observation by Hajek [20] in 2009. In the extraction step, the residual inorganic salts were separated after chilling with methanol. For decolorization of the processed glycerol, a decolorizing agent like activated carbons was used to remove any coloring impurity in the refined glycerol. In the last step of the purification protocol, the refined glycerol was further subjected to vacuum distillation to enhance the extent of the purification [18]. The maximum % age yield of the refined glycerol was achieved at pH1 compared to that obtained at pH 3 and pH 5. At a high pH, for example at pH 5, the removal of inorganic salts was quite difficult due to their incomplete separation [19].

The crude and refined glycerol was found to be blackish brown and light yellow, respectively, comparable to the colors reported by Hunsom [18] in 2013. The pH of the refined glycerol was found to be 6.05 which were comparable to that of 7.03 reported by Manosak et al. [21]. The densities of the crude and refined glycerol were 1.086 and 1.260 g/cm^3, respectively, almost similar to the findings of Yildirim et al. [22]. The refractive index of the refined glycerol was depicted to be 1.47 which was in accordance with 1.473 as reported by Bournay et al. [23]. The Surface tension of the refined glycerol was estimated as 64.7 mN/m at 20 °C. The physico-chemical properties of the glycerol are given in Table 1.

3.2 Experimental Layout and Interpretation of Value

According to the CCRD design, a set of fifty experiments was performed without blocking. The experimental output (% yield of purified glycerol) based on the CCRD is given in Table 2. In each experiment, different levels of reaction variables, *i.e.*, pH, reaction temperature, reaction time, carbon dose,

and rate of stirring, were used in the ranges of 1- 5, 30 - 50 °C, 20 - 60 minutes, 20 - 250 g and 200 - 500 rpm, respectively.

After performing the fifty experiments according to the CCRD (Table 2), the minimum and maximum purified glycerol yields were found to be 49.12% and 83.14%, respectively while the average refined glycerol % yield was 64.38% with a standard deviation of 9.3%.

Table 1. Preliminary physico-chemical properties of crude and refined glycerol.

Physical characters	Crude glycerol Mean±SD	Refined glycerol Mean±SD	Reference value (1)	Reference value (2)	Reference value(3)
pH	9±01	6.05±0.01	5.5	5	7.03
Colour	Blackish brown	Light yellow	Light brown	light yellow	light yellow
Ash content	11.261±5.0	1.05±0.09	0.05	10.80	0.0002-0.0005
Density(g/cm^3)	1.086±0.2	1.260±0.051	1.261	1.254	1.222
Specific gravity	1.337±0.5	1.263±0.01	1.264	1.262	1.2636
Refractive index	1.455±0.01	1.47±0.1	1.472	1.473	1.473
Surface tension (N/m)	24.5±0.03	64.7±0.01	62.50	59.30	65.00

Note: SD means standards deviation

Table 2. Experimental data for central composite response surface second order design.

Run	pH	Time (min)	Temp (°C)	RPM	Carbon dose (g)	%Yield
1	3	40	40	350	135	71.98
2	1	60	50	200	20	83.06
3	1	20	50	500	20	67.12
4	5	60	50	200	20	57.64
5	1	20	50	200	250	66.18
6	3	40	40	350	135	71.98
7	1	60	30	200	20	76.46
8	5	60	30	200	250	53.94
9	1	60	30	200	250	63.14
10	1	20	30	200	20	65.64
11	3	40	40	500	135	59.26
12	5	20	30	500	250	51.38
13	3	40	40	350	135	71.98
14	3	40	30	350	135	69.98
15	1	20	30	500	250	62.52
16	1	60	50	500	20	67.58
17	1	20	50	200	20	72.26
18	5	60	30	500	20	50.00
19	1	20	30	500	20	64.40
20	3	40	40	350	135	71.98
21	3	20	40	350	135	73.56

Table 2. Experimental data for central composite response surface second order design.

Run	pH	Time (min)	Temp (°C)	RPM	Carbon dose (g)	%Yield
22	1	60	50	200	250	79.06
23	3	40	40	350	135	71.98
24	3	40	40	200	135	75.58
25	5	20	30	200	250	53.94
26	3	40	40	350	20	83.14
27	3	40	50	350	135	73.18
28	3	40	40	350	135	71.98
29	3	40	40	350	250	62.58
30	5	20	50	200	20	57.06
31	5	60	50	200	250	55.94
32	1	40	40	350	135	61.64
33	5	40	40	350	135	53.14
34	1	60	30	500	250	62.54
35	3	40	40	350	135	71.98
36	5	20	50	500	250	50.51
37	5	60	30	200	20	56.58
38	5	20	30	200	20	56.52
39	1	20	50	500	250	65.14
40	1	60	30	500	20	65.86
41	1	60	50	500	250	76.04
42	1	20	30	200	250	69.46
43	5	20	50	500	20	53.92
44	5	60	50	500	20	54.04
45	5	60	30	500	250	49.12
46	5	60	50	500	250	50.50
47	3	60	40	350	135	68.54
48	3	40	40	350	135	71.98
49	5	20	30	500	20	53.04
50	5	20	50	200	250	52.08

3.3 Model Fitness and Diagnostic Check

From the data of the model significance, lack of fit, R-square and adjusted R-square values for four models, *i.e.,* quadratic, linear, 2F1 and cubic models, it was depicted that the quadratic model was more significant ($p<0.05$) as compared to the other models. The lack of fit test also recommended that this model was a good fit for the obtained data ($p>0.05$). Even though the cubical model, R^2 (0.9812), and the adjusted R^2 (0.9341) values were higher than the quadratic model; but on the basis of the model significance and lack of fit test, it was recommanded that the quadratic design was the best model for the presentation of the present study design. The normality plot was also a very important parameter that proved the significance of the selected quadratic values.

The residuals p-p plot, Figure 2, showed that all the points lie on the straight line which is the indication that the residuals had a normal

distribution. The presence of an outlier was totally ignored in the p-p plot due to the normal distribution of all points in Figure 2. The plot (Figure 2) of predicted vs. actual residuals also ascertained the fitness of selected quadratic model.

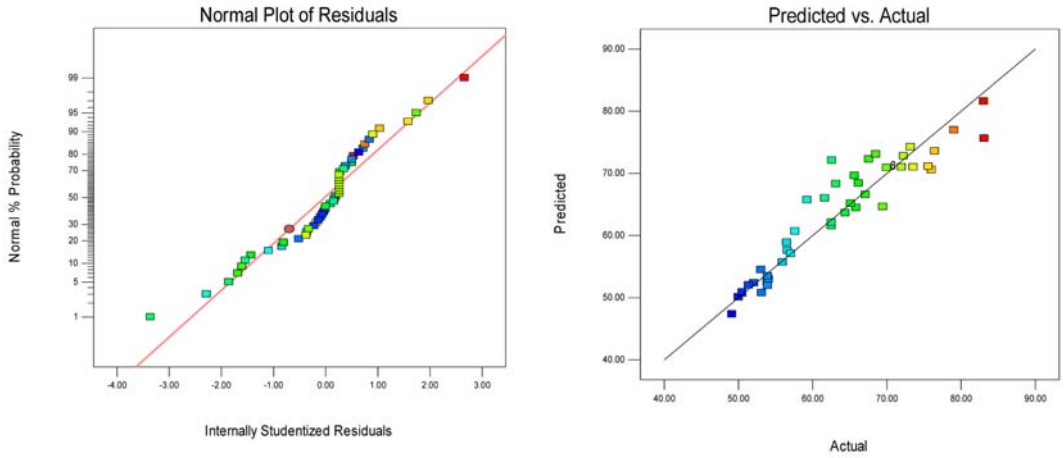

Figure 2. Normal probability and predicted vs actual values.

3.4 Analysis of Variance for Response Surface Quadratic Model

ANOVA Table 3, clearly depicted the significance of selected quadratic model with F-value i.e., 12.63 and *p*-value 0.0001 < 0.05. The lack of fit test was also good for the selected model with *P*-value 0.2588 > 0.05. The adjusted R^2 value revealed that 83. 60 % of the variablity in the refined glycerol yield was due to the controlled variables A, B, C, D and E, whereas the remaing 16.86% variation may have been due to other uncontrollable varaibles. Analysis of variance based on experimental results revealed that the linear terms of the model, *i.e.*, pH during acidification (A), glycerol extraction temperature (C), rate of shaking during extractiion (D) and dose of activated carban for decolorization (E) were found to be significant at 5% level with *p*-values < 0.05, except glycerol extraction time with *p*-value > 0.05. Out of all first order interaction terms, AB, AC and BC were significant at a 10% level. Furthermore, the quadratic terms of pH during acidification (A^2) was found to be significant with *p*-values< 0.05.

3.5 Response Surface Plots

Fundamentally, response surface methodology is a technique which covers both the field of statistics and mathematics. Response surface methodology is commonly used for development, improvement and optimization purposes. The most applicable and important applications of response surface methodology are in industries and laboratory work, where several parameters influence the quality, % yield of the product and process, respectively. By using response surface methodology, the characteristics of the prepared product can be analyzed and compared to the reference sample [22].

All the response surface plots showing the impact of various first order interaction terms on the % yield of the refined glycerol depicted the optimum levels of glycerol purification, hence, high yield can be obtained by performing glycerol purification at the

following optimum reaction conditions, *i.e.* pH (1), rate of shaking (200 rpm), glycerol extraction time (60 minutes), glycerol extraction temperature (50 °C) and dose of activated carbon (20g for 50g of crude glycerol sample) (Figure 3).

The yield of the refined glycerol under optimized conditions was found to be 83.60%. Furthermore, it is observed that any fluctuation in the above mentioned optimized conditions will result in a lower % yield of refined glycerol.

Table 3. Analysis of variance (ANOVA) of central composite response surface second order quadratic model.

Source	Sum of square	df	Mean square	F-value	p-value
Model	3841.64	20	192.08	12.63	0.0001
A-pH during acidification	1969.62	1	1969.62	129.55	0.0001
B- Glycerol extraction time	36.73	1	36.73	2.41	0.13
C-Glycerol extraction temperature	94.75	1	94.75	6.23	0.018
D- Rate of shaking during extraction	246.78	1	246.78	16.23	0.0004
E-Dose of activated carbon	106.73	1	106.73	7.02	0.01
AB	54.28	1	54.28	3.57	0.06
CD	0.084	1	0.084	0.0055	0.94
CE	0.858	1	0.858	0.056	0.81
AC	48.21	1	48.21	3.17	0.08
AD	5.15	1	5.15	0.33	0.56
AE	0.29	1	0.29	0.01	0.88
BC	47.23	1	47.23	3.10	0.08
BD	19.53	1	19.53	1.28	0.26
BE	0.151	1	0.151	0.0099	0.92
A^2	393.55	1	393.55	25.88	0.0001
B^2	2.70	1	2.70	0.17	0.67
C^2	6.14	1	6.14	0.40	0.53
D^2	16.51	1	16.51	1.08	0.30
E^2	20.17	1	20.17	1.32	0.26
Residual	440.89	29	15.20		
Lack of Fit	440.89	22	20.04		
Pure Error	0	7	0		

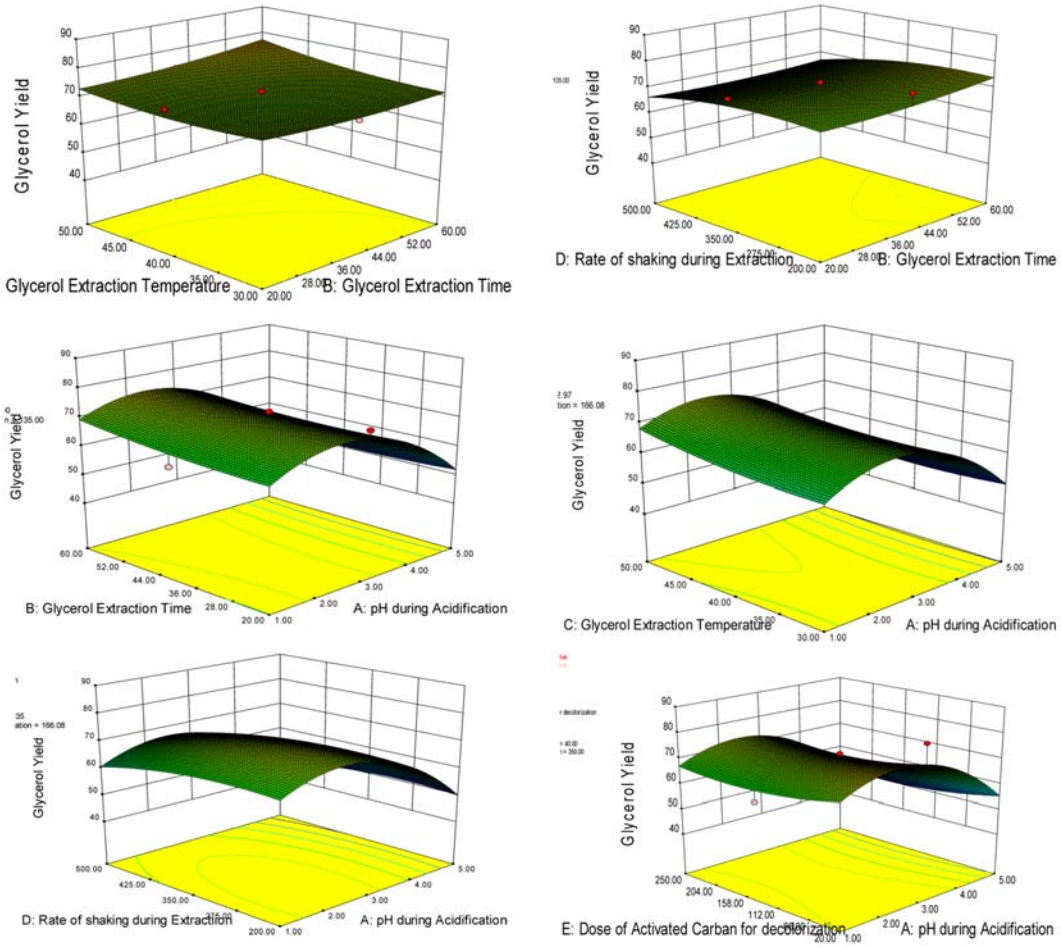

Figure 3. Response surface plots showing the impact of first order interaction terms on % yield of refined glycerol.

3.6 FTIR Analysis of Glycerol

The FTIR spectrum of the crude glycerol was complex (Figure 4) showing peaks of several functional groups. O-H stretching frequency was observed at 3321.78 cm^{-1} while a strong peak at 1739.61 cm^{-1} was due to the C=O stretching of esters present in the crude glycerol. O-H bending was observed at 910.22 cm^{-1}, while the COO group related to soap impurities showed a peak at 1548.80 cm^{-1}, representing dissolved salts in the crude glycerol. A peak at 3009.99 cm^{-1} could be attributed to C=C present in the alkyl part of the fatty acid chain [18]. FTIR spectrum of the refined glycerol is shown in Figure 5. From the spectrum, it was depicted that the functional groups present in this spectrum were alike to those described in literature. The FTIR spectrum of the refined glycerol showed O-H stretching at 3265 cm^{-1} while C-H stretching was revealed by the peaks in the region of 2810-2950 cm^{-1}. The C=O stretching band present in the crude glycerol at 1655 cm^{-1} was absent in the refined glycerol spectra. The peak at 1560 cm^{-1} was also absent in the refined glycerol indicating the removal of the salts. Bending of the C-O-H group was also observed in the region of 1400 to 1420 cm^{-1} of the C-O stretching of the primary alcohol,

which is shown at 1112 cm^{-1}.

3.7 Raman Spectroscopic Analysis of Glycerol

In the Raman spectrum of the refined glycerol, the Raman line at 799-815 cm^{-1} was due to the presence of -C-C- skeletal stretching in $-(CH_2)_n-$ (Table 4). The vibrations from the glycosidic linkage are shown in the form of the Raman line in the range of 850-990 cm^{1} as depicted by Berg and Otero [24]. The presence of the in-phase methylene (CH_2) twisting motion was revealed by the presence of the Raman line approximately at 1318 and 1450 cm^{-1} (Figure 6 and 7).

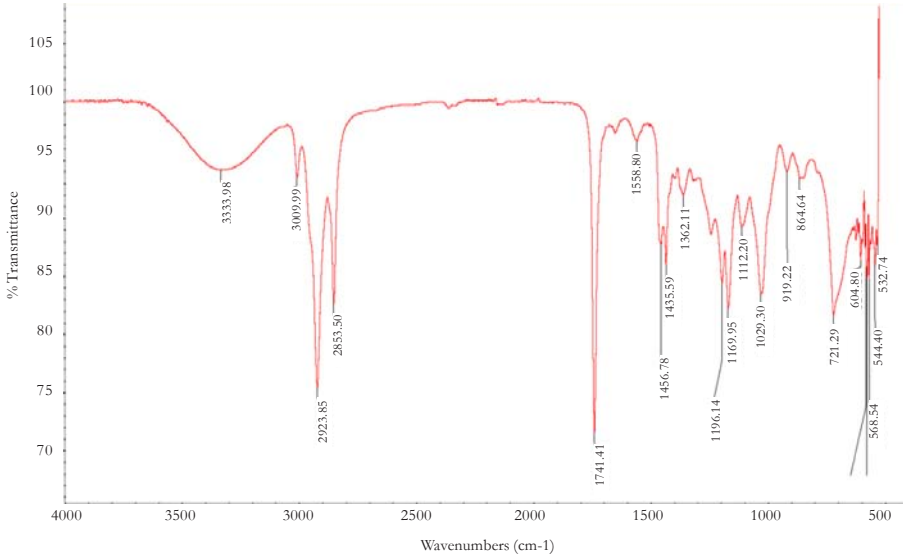

Figure 4. IR Spectrum of crude glycerol.

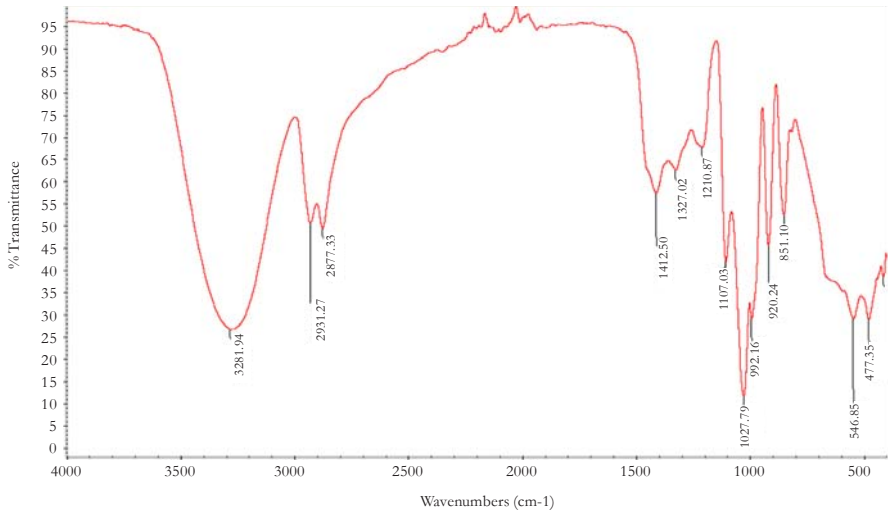

Figure 5. IR Spectrum of refined glycerol.

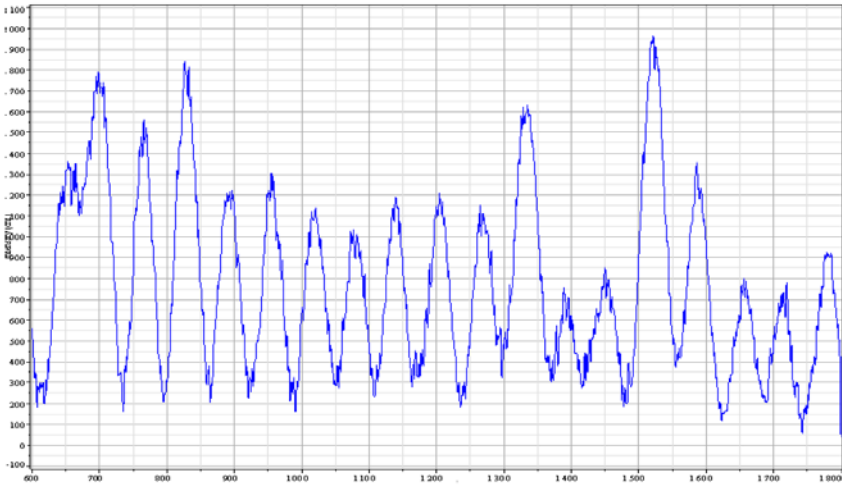

Figure 6. Raman spectrum of crude glycerin.

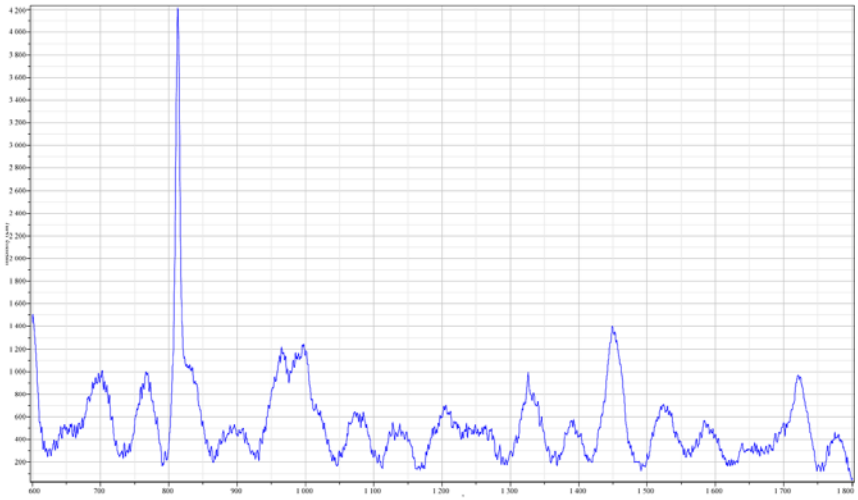

Figure 7. Raman spectrum of refined glycerin.

Table 4. Characteristics Raman peaks and their position.

Raman shift (cm^{-1}) approximately	Characteristics Raman peaks and their position
799-815 cm^{-1}	Incidence of -C-C- skeletal stretching in -(CH_2)n
850-990 cm^{-1}	Vibrations from the glycoside linkage
1200-1500 cm^{-1}	Distinctive vibrations
1318 cm^{-1}	In-phase methylene (CH_2) twisting motion
1450 cm^{-1}	CH_2 scissoring mode of the saturated fatty acid part.

4. CONCLUSIONS

Purification of the under study crude glycerol was carried out using response surface methodology (RSM) that proved to be a very emphatic statistical tool for the optimized purification of crude glycerol. The optimum conditions as per said statistical optimization tool were found to be pH (1), rate of shaking (200 rpm), glycerol extraction time (60 min), glycerol extraction temperature (50 °C) and dose of activated carbon (20 g for 50 g of crude glycerol sample) resulting in the optimal yield of refined glycerol, *i.e.*, 83.60 %. Hence, the reported optimal conditions for optimum purification of residual glycerol has potential future benefits to make the biodiesel production process cost effective by further transforming the refined glycerol into other valuable byproducts.

REFERENCES

[1] Alhassan F.H., Yunus R., Rashid U., Sirat K., Islam A., Lee H.V. and Taufiq-Yap Y.H., *Appl. Catal. Gen.,* 2013; **456**: 182-187. DOI 10.1016/j.apcata.2013.02.019.

[2] Isahak W.N.R.W., Ramli Z.A.C., Ismail M., Jahim J.M. and Yarmo M.A., *Sep. Purif. Rev.,* 2015; **44**: 250-267. DOI 10.1080/15422119.2013.851696.

[3] Rashid U., Ibrahim M.,Yasin S., Yunus R., Taufiq-Yap Y.H. and Knothe G., *Ind. Crop. Prod.*, 2013; **45**: 355-359. DOI 10.1016/j.indcrop.2012.12.039.

[4] Nehdi I.A., Sbihi H.M., Mokbli S., Rashid U. and Al-Resayes S.I., *Ind. Crop. Prod.*, 2015; **69**: 257-262. DOI 10.1016/j.indcrop.2015.02.029.

[5] Mumtaz M., Adnan A., Anwar F., Mukhtar H., Raza M., Ahmad F. and Rashid U., *Energies*, 2012; **5**: 3307-3328. DOI 10.3390/en5093307.

[6] Asad-ur-Rehman A., Saman W.R.G., Nomura N., Sato S. and Matsumura M., *J. Chem. Technol. Biotechnol.*, 2008; **83**: 1072-1080. DOI 10.1002/jctb.1917.

[7] Mu Y., Teng H., Zhang D.J., Wang W. and Xiu Z.L., *Biotechnol. Lett.*, 2006; **28**: 1755-1759. DOI 10.1007/s10529-006-9154-z.

[8] Arzamendi G., Campo I., Arguinarena E., Sanchez M., Montes M. and Gandia L.M., *Chem. Eng. J.*, 2007; **134**: 123-130. DOI 10.1016/j.cej.2007.03.049.

[9] Tan H.W., Aziz A.R.A. and Aroua M.K., *Sustain. Energ. Rev.*, 2013; **27**: 118-127. DOI 10.1016/j.rser.2013.06.035.

[10] Thompson J.C. and He B.B., *Appl. Eng. Agric.*, 2006; **22**: 261-265. DOI 10.13031/2013.20272.

[11] Yang F., Hanna M.A. and Sun R., *Biotechnol. Biofuel.,* 2012; **5**: 1-10. DOI 10.1186/1754-6834-5-13.

[12] Behr A., Eilting J., Irawadi K., Leschinski J. and Lindner F., *Green Chem.*, 2008; **10**: 13-30. DOI 10.1039/B710561D.

[13] Lin L., Cunshan Z., Vittayapadung S., Xiangqian S. and Mingdong D., *Appl. Energ.*, 2011; **88**: 1020-1031. DOI 10.1016/j.apenergy.2010.09.029.

[14] Zhou C.H., Beltramini J.N., Fan Y.X. and Lu G.Q., *Chem. Soc. Rev.,* 2008; **37**: 527-549. DOI 10.1039/B707343G.

[15] Johnson D.T. and Taconi K.A., *Environ. Prog.* 2007; **26**: 338-348. DOI 10.1002/ep. 10225.

[16] Pott R.W., Howe C.J. and Dennis J.S., *Bioresour. Technol.*, 2014; **152**: 464-470. DOI 10.1016/j.biortech.2013.10.094.

[17] Nanda M.R., Yuan Z., Qin W., Poirier M.A. and Chunbao X., *Austin J. Chem. Eng.,* 2014; **1**: 01-07.

[18] Hunsom M., Saila P., Chaiyakam P. and Kositnan W., *Int. J. Renew. Energ. Res.,* 2013; **3**: 2.

[19] Wall J., Van J. and Thompson J., *Am. Soc. Agric. Biol. Eng.,* 2011; **54**: 535-541.

[20] Hajek M. and Skopal F., *Proceeding of the 44th International Petroleum Conference*, Bratislava, Slovak Republic, September 21-22, 2009.

[21] Manosak R., Limpattayanate S. and Hunsom M., *Fuel Proc. Technol.,* 2011; **92**: 92-99. DOI 10.1016/j.fuproc.2010.09.002.

[22] Yildirim O., Kiss A. and Kenig Y., *Sep. Purif. Technol.,* 2011; **80**: 403-417. DOI 10.1016/j.seppur.2011.05.009.

[23] Bournay L., Casanave D., Delfort B., Hillion G. and Chodorge J.A., *Catal. Today,* 2005; **106**: 190-192. DOI 10.1016/j.cattod.2005.07.181.

[24] Berg R.W. and Otero A.D., *Vib. Spectrosc.*, 2006; **42**: 222-225. DOI 10.1016/j.vibspec.2006.05.031.